

Eccentric Early Migration of Neptune

David Nesvorný

*Department of Space Studies, Southwest Research Institute,
1050 Walnut St., Suite 300, Boulder, CO, 80302, USA*

ABSTRACT

The dynamical structure of the Kuiper belt can be used as a clue to the formation and evolution of the Solar System, planetary systems in general, and Neptune’s early orbital history in particular. The problem is best addressed by forward modeling where different initial conditions and Neptune’s orbital evolutions are tested, and the model predictions are compared to orbits of known Kuiper belt objects (KBOs). It has previously been established that Neptune radially migrated, by gravitationally interacting with an outer disk of planetesimals, from the original radial distance $r \lesssim 25$ au to its current orbit at 30 au. Here we show that the migration models with a very low orbital eccentricity of Neptune ($e_N \lesssim 0.03$) do not explain KBOs with semimajor axes $50 < a < 60$ au, perihelion distances $q > 35$ au and inclinations $i < 10^\circ$. If $e_N \lesssim 0.03$ at all times, the Kozai cycles control the implantation process and the orbits with $q > 35$ au end up having, due to the angular momentum’s z -component conservation, $i > 10^\circ$. Better results are obtained when Neptune’s eccentricity is excited to $e_N \simeq 0.1$ and subsequently damped by dynamical friction. The low- e & low- i orbits at 50-60 au are produced in this model when KBOs are lifted from the scattered disk by secular cycles – mainly the apsidal resonance ν_8 – near various mean motion resonances. These results give support to a (mild) dynamical instability that presumably excited the orbits of giant planets during Neptune’s early migration.

Subject headings:

1. Introduction

Previous studies of Kuiper belt formation envisioned dynamical models where Neptune maintained a very low orbital eccentricity, comparable to the present $e_N \simeq 0.01$, during

its early migration (e.g., Malhotra 1993, 1995; Hahn & Malhotra 2005; Gomes 2003). An instability model was subsequently suggested to explain the somewhat excited orbits of the outer planets (Tsiganis et al. 2005). In the original instability model, Neptune was scattered to a highly eccentric orbit ($e_N \gtrsim 0.2$) that briefly overlapped with the Kuiper belt (e.g., Levison et al. 2008, Morbidelli et al. 2008, Gomes et al. 2018). Different arguments have been proposed in the past to rule out specific migration/instability regimes (e.g., Batygin et al. 2011, Wolff et al. 2012, Dawson & Murray-Clay 2012). For example, the *high*-eccentricity instability model with fast (~ 1 Myr) subsequent circularization of Neptune’s orbit does not reproduce the generally wide inclination distribution of KBOs, because there is not enough time to excite the orbital inclinations in this model (Nesvorný 2015). Most modern studies of the instability therefore considered $e_N \sim 0.1$ (e.g., Nesvorný & Morbidelli 2012; Kaib & Sheppard 2016; Deienno et al. 2017, 2018; Clement et al. 2020).

Here we highlight a new constraint that could be used to rule out the very-*low*-eccentricity migration of Neptune ($e_N \lesssim 0.03$). The Outer Solar System Origins Survey (OSSOS; Bannister et al. 2018) identified a population of KBOs with semimajor axes $50 < a < 60$ au, perihelion distances $q > 35$ au and inclinations $i < 10^\circ$. We show that this population can easily be explained if Neptune reached eccentricity $e_N \simeq 0.1$ during migration, perhaps due to its interaction with Uranus or a rogue planet (e.g., Nesvorný 2011). In this model, bodies starting at $r \lesssim 30$ au are scattered by Neptune to orbits with $50 < a < 60$ au and $q \sim 30$ au, where they interact with various Neptune’s mean motion resonances. The secular cycles, mainly associated with the ν_8 resonance ($g = g_8$, where g and g_8 are the apsidal precession frequencies of a KBO and Neptune, respectively), then act to decouple the scattered KBOs from Neptune and produce orbits with $50 < a < 60$ au and $q > 35$ au. As the ν_8 resonance leaves orbital inclinations unchanged, many of these bodies keep their initially low inclinations and end up with $i < 10^\circ$, thus explaining the existence of high- q and low- i KBOs with $50 < a < 60$ au.

If, instead, $e_N \lesssim 0.03$ during Neptune’s migration, the ν_8 resonance is not effective and scattered KBOs decouple from Neptune – in absence of other external perturbations – by the Kozai resonance (Kozai 1962; more specifically: by the Kozai resonance *inside* various mean motion resonances with migrating Neptune, see below). As the quantity $\sqrt{1 - e^2} \cos i$ is preserved during Kozai cycles, lowering the orbital eccentricity means that the inclination

must increase. We find that this leads to a situation where bodies cannot reach the orbits with $50 < a < 60$ au, $q > 35$ au and $i < 10^\circ$, and use this result to argue against the very-low-eccentricity migration of Neptune. Alternatively, the KBOs with $50 < a < 60$ au, $q > 35$ au and $i < 10^\circ$ could have originated in a hypothetical, low- e and low- i disk at $50 < r < 60$ au that was subsequently disturbed by some process. We also discuss migration models with an elevated orbital inclination of Neptune, where the ν_{18} resonance ($s = s_8$, where s and s_8 are the nodal precession frequencies of a KBO and Neptune, respectively) would affect orbital inclinations.

2. Data, Model and Results

The orbits of KBOs with $50 < a < 60$ au are shown in Fig. 1. OSSOS detected 52 KBOs in this region. There is a cluster of objects with $q < 35$ au in the 5:2 resonance ($a \simeq 55.4$ au; Malhotra et al. 2018). The 5:2 resonance was previously shown to host a large population of KBOs that can rival that of the 3:2 resonance (Gladman et al. 2012). This is not the subject of the present paper. Here we focus on the population of KBOs with $q > 35$ au. There are 25 OSSOS bodies with $50 < a < 60$ au and $q > 35$ au, of which 14 are classified by the OSSOS team as detached; the rest is classified as resonant (see Gladman et al. 2008 for a definition of different dynamical categories). The detached orbits are expected to be stable on long time intervals. We integrated all 25 OSSOS bodies with $50 < a < 60$ au and $q > 35$ au and found that most of their orbits remain practically unchanged over 4.5 Gyr.¹ This means that a great majority of these bodies must have evolved onto their current orbits during Neptune’s early migration. For comparison, of the 27 OSSOS bodies with $50 < a < 60$ au and $q < 35$ au, 20 are resonant (mainly the 5:2 resonance), six are scattering and one as detached. This shows that $q = 35$ au is a good division line, at least for $50 < a < 60$ au, between objects coupled to Neptune and those that are not.

¹It is not clear whether the orbits are known well enough to be able to conclusively establish their long term stability. For example, the semimajor axis uncertainties are typically 0.002-0.04 au, which can matter if some of the orbits are very close to mean motion resonances. Five objects – 2013 JH64, 2014 UG228, 2015 KT174, 2015 KV174, 2015 RU278 – were scattered by Neptune and removed from the simulation. Of these, only 2014 UG228 has low orbital inclination ($i = 3.5^\circ$).

The inclination distribution of known KBOs with $50 < a < 60$ au and $q > 35$ au is relatively wide with many orbits having $i < 10^\circ$ (10 of 25, or 40%; Fig. 2). Of these, five bodies are classified as resonant (two in 13:6, one in each 7:3, 8:3, 13:5, none in 5:2) and five as detached. The orbital eccentricities are too large for these bodies to accrete on their current orbits. They must have formed elsewhere and evolved onto current orbits early in the solar system history. Here we show how this constrains Neptune’s migration.

The model results shown in Fig. 2 were taken from Nesvorný et al. (2020), where we conducted simulations of Neptune’s early migration. Specifically, the results in Fig. 2a correspond to the s10/30j model (see Table 1 in Nesvorný et al. 2020) where Neptune migrated from $a_{N,0} = 24$ au to $a_{N,0} = 27.7$ au in the first 10 Myr, before its orbit was excited to $e_N = 0.1$ during the dynamical instability. Neptune’s eccentricity was then slowly damped as Neptune migrated toward 30 au. The results in Fig. 2b correspond to the s30/100j model with a longer migration timescale and $e_N = 0.1$. In both models, Neptune’s orbital inclination remained near its current value. We find that bodies are implanted onto orbits with $50 < a < 60$ au, $q > 35$ au and $i < 10^\circ$ by a combined effect of Neptune scattering, mean motion resonances and ν_8 .

In the example shown in Fig. 3, taken from s10/30j with $e_N = 0.1$, the test body started below 30 au and was scattered by Neptune to $a \simeq 52$ au and $q \simeq 30$ au at $t \simeq 33.2$ Myr after the start of our simulation (panel a). It evolved onto an orbit with a very large libration amplitude in the 7:3 mean motion resonance with Neptune (panels b and h). The secular resonance ν_8 (panel e) acted to decrease the orbital eccentricity (panels c), and the orbit was decoupled from Neptune. It was subsequently released from the 7:3 resonance and ended up on a stable orbit with $q \simeq 38$ au and $i \simeq 1^\circ$. We inspected 40 orbital histories of bodies that evolved onto the orbits with $50 < a < 60$ au, $q > 35$ au and $i < 10^\circ$ in the s10/30j and s30/100j migration models and found that the ν_8 resonance plays the dominant role in decoupling bodies from Neptune (most orbital evolutions are more complicated than the one shown in Fig. 3; different mean motion resonances are involved). As the ν_8 resonance does not affect orbital inclinations, orbits can maintain their low inclinations as they evolve from the scattered orbits to $q > 35$ au.

We now compare the model distributions obtained in the s10/30j and s30/100j models with the OSSOS observations (Fig. 2). This is not an apple-to-apple comparison because the

model represents an intrinsic orbital distribution, whereas the data are affected by observational biases (e.g., flux biases, pointing history, rate cuts and object leakage; Bannister et al. 2016). But that’s not the point here. The point is that the migration model with $e_N \simeq 0.1$ is capable of producing orbits with $50 < a < 60$ au, $q < 35$ au and $i < 10^\circ$ in the first place, and thus provides a straightforward explanation for this population. A detailed comparison with the OSSOS observations will require certain assumptions about the magnitude distribution of KBOs and the use of the OSSOS simulator (Lawler et al. 2018). This is left for future work. Here we just point out the orbits with low inclinations are preferentially picked up by the OSSOS observations near the ecliptic.

Figure 4 shows the results of the migration models where Neptune’s eccentricity stayed low at all times ($e_N \simeq 0-0.02$; no instability, otherwise identical to the s10/30j and s30/100j models discussed above). The model distributions are markedly different from the ones shown in Fig. 2. To understand this difference, note that the ν_8 resonance becomes ineffective when Neptune’s eccentricity is low (e.g., Morbidelli 2002, Sect. 11.2.3). This means that bodies cannot be decoupled from the scattered orbits by ν_8 . Instead, slower chaotic effects and the Kozai resonance come into action (Kozai 1962; see Sect. 11.2.2 in Morbidelli 2002 for the Kozai resonance *inside* mean motion resonances). The Kozai resonance was present in the models with $e_N = 0.1$ as well but there the decoupling mechanism was controlled by the stronger ν_8 resonance.

With ν_8 gone for $e_N \simeq 0$, the orbits affected by Kozai cycles conserve the z component of the (scaled) angular momentum, $L_z = \sqrt{1 - e^2} \cos i$. Thus, as the eccentricity is driven down during the decoupling process, the inclination must go up. An example of this evolution is shown in Fig. 5. This effectively defines an excluded region in the (q, i) plane that cannot be reached by the decoupled orbits (even if they start on the scattered orbits with $i = 0$).² Indeed, the model orbits do not evolve into this region if $e_N \simeq 0-0.02$ (Fig. 4).

This is the heart of our argument: the observed orbits with $50 < a < 60$ au, $q > 35$ au and $i < 10^\circ$ cannot be explained in the migration model with $e_N \simeq 0-0.02$. Their

²In addition, in the absence of strong ν_8 -resonance effects, the efficiency of the decoupling process drops. This then leads to a much smaller population of detached objects than in the models with $e_N \simeq 0.1$ (compare Figs. 2 and 4). The bodies that eventually evolve to $q > 35$ au spend longer time on the Neptune-crossing orbits and tend to have larger inclinations. This further emphasizes the difference between Figs. 2 and 4.

existence implies that the ν_8 resonance was effective during Neptune’s migration, rules out the migration model with $e_N \simeq 0-0.02$, and gives support to the models with (mild) dynamical instabilities ($e_N \simeq 0.1$; e.g., Nesvorný 2011, Nesvorný & Morbidelli 2012).³ To get better hold of the critical eccentricity of Neptune implied by this argument, we performed two additional simulations: (i) s10/30j with $e_N = 0.03$, and (ii) another one with shorter migration timescales ($\tau = 5$ and 10 Myr, see Nesvorný et al. 2020 for a definition of these parameters) and $e_N = 0.1$. The results of (i) are similar to the case with $e_N = 0-0.02$, which allows us to estimate the critical eccentricity $e_N \sim 0.05$. From (ii), we speculate that the critical eccentricity may show a weak dependence on the timescale of Neptune’s migration with shorter timescales implying slightly larger thresholds.

3. Discussion

Arguments similar to those described above can be made based on the orbits of detached orbits with $a > 60$ au. We are less confident in drawing inferences from that population, because: (1) the population of detached bodies with $a > 60$ au is still relatively small, and (2) it may have been affected by stellar encounters, planet 9, or other external perturbations not included in our model. We thus leave a careful study of that population for future work. As for $a < 50$ au, the observed KBOs are thought to be a mixture of dynamically ‘cold’ ($i < 5^\circ$) and ‘hot’ populations ($i > 5^\circ$), respectively representing planetesimals that formed at $r \simeq 42-47$ au (i.e., between the 3:2 and 2:1 resonances with Neptune) and $r < 30$ au (i.e., below the current orbit of Neptune; see Morbidelli & Nesvorný 2020 for a review). It is difficult to build a case on this population, because most of the low- i bodies found there did not evolve through the scattered disk. Instead, they were born and survived with $40 < a < 47$ au and $i < 5^\circ$.

This raises a question whether the observed population of KBOs with $50 < a < 60$ au, $q > 35$ au and $i < 10^\circ$ could simply be a continuation of the cold disk from below the 2:1 resonance to $r > 50$ au. The main argument against this possibility is that the cold KBOs at $r \simeq 42-47$ au remained with $i < 5^\circ$. If the same population existed beyond 50 au, it would

³See Nesvorný et al. (2020) for other KBO populations obtained in the model with $e_N = 0.1$.

preferentially be seen by OSSOS (which is strongly biased, due to its observing strategy, toward discovering objects with $i \sim 0$). The orbits with $50 < a < 60$ au instead have a broad inclination distribution and do not show any hint of bimodality seen inward of the 2:1 resonance. Perhaps, then, some unknown dynamical mechanism (3:1 resonance?, rogue planets?) have strongly excited the orbits starting with $50 < a < 60$ au and $e \sim i \sim 0$. In that case, however, it would have to be demonstrated that the mechanism can excite orbital inclinations for $a > 50$ au but leave $i < 5^\circ$ for $40 < a < 47$ au.

The detached orbits can potentially be generated from the scattering disk by rogue planets scattered off of Neptune (Gladman & Chan 2006). For this to happen, the largest rogue planet would need to have mass $\gtrsim 1 M_{\text{Earth}}$, where M_{Earth} is the Earth mass (Gladman & Chan 2006). Shannon & Dawson (2018) placed an upper limit on the number of Earth-mass planets in the original outer disk. From the preservation of ultra wide KBO binaries they found that < 3 Earth-mass planets could have been initially present (68% statistical probability), and from the low orbital inclinations of cold classicals they found < 1 Earth-mass planets (68% probability). Only a fraction of these planets would be scattered outward by Neptune and could contribute to the construction of the detached disk. Unfortunately, detailed predictions of the rogue-planet model for the orbital distribution of KBOs at 50-60 au are not available at this moment.

Additional possibility is related to the effects of the ν_{18} resonance. Volk & Malhotra (2019) showed that ν_{18} can increase the orbital inclinations of bodies implanted in the 3:2 resonance, if Neptune’s inclination was somewhat elevated above its current value (proper $i_N \simeq 0.7^\circ$). If that’s the case, assuming $e_N \sim 0$ and large i_N , we speculate that the ν_{18} resonance (near and inside various mean motion resonances; see Nesvorný & Roig 2000, 2001; Volk & Malhotra 2019) may have scrambled the inclination distribution of bodies with $q > 35$ au. This could potentially change the inclination distribution and explain the observed KBO population with $50 < a < 60$ au, $q > 35$ au and $i < 10^\circ$. It is unknown, however, what could cause high i_N and leave low e_N during Neptune’s migration, because mean motion resonances and/or scattering tend to excite e_N .

Finally, as an important caveat, we emphasize that our exploration of parameter space is incomplete. In the simulations presented here, we varied Neptune’s eccentricity ($e_N = 0, 0.03$ and 0.1) and the migration/damping timescales ($\tau = 5\text{-}10, 10\text{-}30$ and $30\text{-}100$ Myr).

We did not test the dependence on other parameters, such as i_N (see the discussion above), the relative position of planets during migration, etc. For example, the location of the ν_8 resonance can be sensitive, in general, to the detailed configuration of planets. The ν_8 resonance, however, always occurs near and inside of mean motion resonances with Neptune where the apsidal precession rate of orbits has a singularity (Knežević et al. 1991). Thus, given that the implantation mechanism identified here relies on the proximity to a mean motion resonance, the detailed behavior of planets should be inconsequential for the main argument presented in this work.

4. Conclusions

We find that the population of KBOs with $50 < a < 60$ au, $q > 35$ au and $i < 10^\circ$ can be explained if Neptune’s orbit was excited to $e_N \simeq 0.1$ during planetary migration and subsequently dumped to the current $e_N = 0.01$ by dynamical friction. If, instead, Neptune maintains a very low orbital eccentricity, $e_N \lesssim 0.03$, at all times, these low- i KBOs are not obtained in the simulations. Our results can be interpreted to give support for a dynamical instability in the early outer solar system. Questions remain, however, related to the cause and orbital behavior of planets during the instability.

The gravitational interaction of Uranus and Neptune, mainly when these planets cross a mutual mean motion resonance during their migration, can excite Neptune’s eccentricity but it is uncommon for this process to generate $e_N > 0.05$. The planetary encounters between ice giants, with Neptune being scattered off of a rogue planet, lead to $e_N \sim 0.1$ quite often (Nesvorný 2011, Nesvorný & Morbidelli 2012, Batygin et al. 2012). The planetary encounters of Neptune with Jupiter or Saturn typically lead to $e_N \gtrsim 0.2$ (Tsiganis et al. 2005, Levison et al. 2008), but this model struggles to match other constraints (e.g., Nesvorný & Morbidelli 2012, Nesvorný 2015). From these considerations, we favor the mild instability model with a large rogue planet.

The work of D.N. was supported by the NASA Emerging Worlds program. We thank the anonymous reviewer for helpful comments on the submitted manuscript.

REFERENCES

- Bannister, M. T., Kavelaars, J. J., Petit, J.-M., et al. 2016, *AJ*, 152, 70. doi:10.3847/0004-6256/152/3/70
- Bannister, M. T., Gladman, B. J., Kavelaars, J. J., et al. 2018, *ApJS*, 236, 1 8
- Batygin, K., Brown, M. E., & Fraser, W. C. 2011, EPSC-DPS Joint Meeting 2011, 1154
- Batygin, K., Brown, M. E., & Betts, H. 2012, *ApJ*, 744, L3. doi:10.1088/2041-8205/744/1/L3
- Clement, M. S., Raymond, S. N., Kaib, N. A., et al. 2020, AAS/Division for Planetary Sciences Meeting Abstracts
- Dawson, R. I. & Murray-Clay, R. 2012, *ApJ*, 750, 43. doi:10.1088/0004-637X/750/1/43
- Deienno, R., Morbidelli, A., Gomes, R. S., et al. 2017, *AJ*, 153, 153. doi:10.3847/1538-3881/aa5eaa
- Deienno, R., Izidoro, A., Morbidelli, A., et al. 2018, *ApJ*, 864, 50. doi:10.3847/1538-4357/aad55d
- Gladman, B. & Chan, C. 2006, *ApJ*, 643, L135. doi:10.1086/505214
- Gladman, B., Marsden, B. G., & Vanlaerhoven, C. 2008, *The Solar System Beyond Neptune*, 43
- Gladman, B., Lawler, S. M., Petit, J.-M., et al. 2012, *AJ*, 144, 23. doi:10.1088/0004-6256/144/1/23
- Gomes, R. S. 2003, *Icarus*, 161, 404. doi:10.1016/S0019-1035(02)00056-8
- Gomes, R., Nesvorný, D., Morbidelli, A., et al. 2018, *Icarus*, 306, 319. doi:10.1016/j.icarus.2017.10.018
- Hahn, J. M., & Malhotra, R. 2005, *AJ*, 130, 2392
- Kaib, N. A. & Sheppard, S. S. 2016, *AJ*, 152, 133. doi:10.3847/0004-6256/152/5/133

- Knežević, Z., Milani, A., Farinella, P., et al. 1991, *Icarus*, 93, 316. doi:10.1016/0019-1035(91)90215-F
- Kozai, Y. 1962, *AJ*, 67, 591. doi:10.1086/108790
- Lawler, S. M., Kavelaars, J. J., Alexandersen, M., et al. 2018, *Frontiers in Astronomy and Space Sciences*, 5, 14. doi:10.3389/fspas.2018.00014
- Levison, H. F., Morbidelli, A., Van Laerhoven, C., et al. 2008, *Icarus*, 196, 258. doi:10.1016/j.icarus.2007.11.035
- Malhotra, R. 1993, *Nature*, 365, 819. doi:10.1038/365819a0
- Malhotra, R. 1995, *AJ*, 110, 420. doi:10.1086/117532
- Malhotra, R., Lan, L., Volk, K., et al. 2018, *AJ*, 156, 55. doi:10.3847/1538-3881/aac9c3
- Morbidelli, A. 2002, *Modern celestial mechanics : aspects of solar system dynamics*, by Alessandro Morbidelli. London: Taylor & Francis, 2002, ISBN 0415279399
- Morbidelli, A., Levison, H. F., & Gomes, R. 2008, *The Solar System Beyond Neptune*, 275
- Morbidelli, A. & Nesvorný, D. 2020, *The Trans-Neptunian Solar System*, 25. doi:10.1016/B978-0-12-816490-7.00002-3
- Nesvorný, D. 2011, *ApJ*, 742, L22. doi:10.1088/2041-8205/742/2/L22
- Nesvorný, D. 2015, *AJ*, 150, 73. doi:10.1088/0004-6256/150/3/73
- Nesvorný, D. & Roig, F. 2000, *Icarus*, 148, 282. doi:10.1006/icar.2000.6480
- Nesvorný, D. & Roig, F. 2001, *Icarus*, 150, 104. doi:10.1006/icar.2000.6568
- Nesvorný, D. & Morbidelli, A. 2012, *AJ*, 144, 117. doi:10.1088/0004-6256/144/4/117
- Nesvorný, D., Vokrouhlický, D., Alexandersen, M., et al. 2020, *AJ*, 160, 46. doi:10.3847/1538-3881/ab98fb
- Shannon, A. & Dawson, R. 2018, *MNRAS*, 480, 1870. doi:10.1093/mnras/sty1930

Tsiganis, K., Gomes, R., Morbidelli, A., et al. 2005, *Nature*, 435, 459.
doi:10.1038/nature03539

Volk, K., & Malhotra, R. 2019, *AJ*, 158, 64

Wolff, S., Dawson, R. I., & Murray-Clay, R. A. 2012, *ApJ*, 746, 171. doi:10.1088/0004-637X/746/2/171

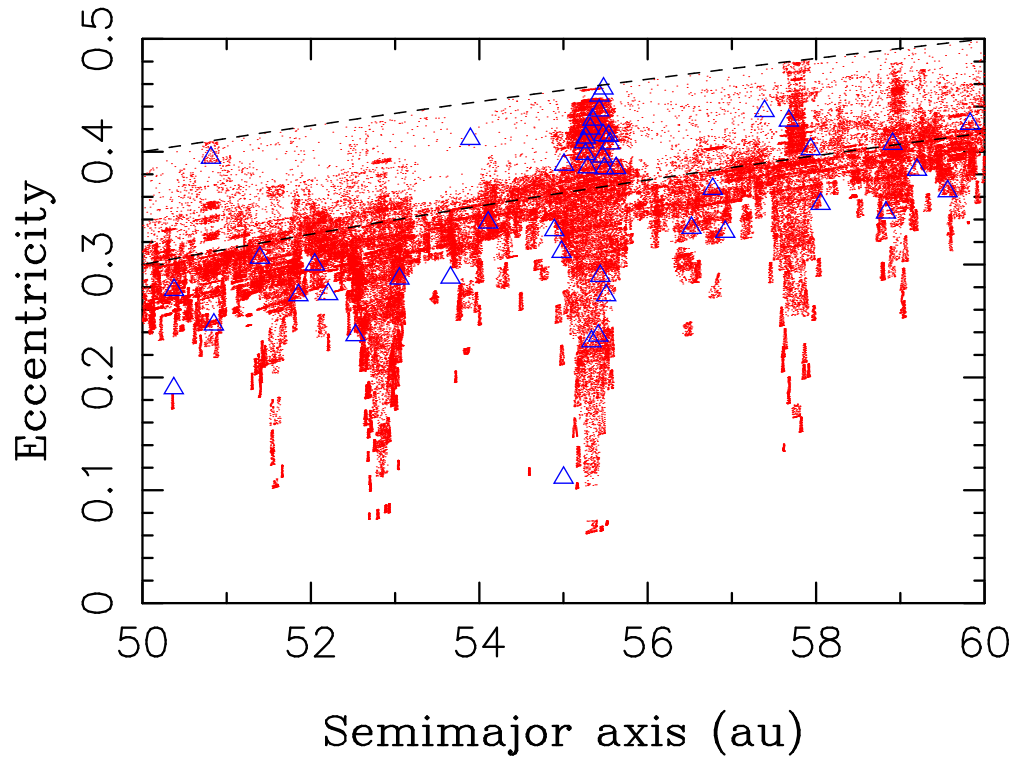


Fig. 1.— The orbits of KBOs with $50 < a < 60$ au: the model orbits from s10/30j (Nesvorný et al. 2002, $e_N = 0.1$; red dots) and OSSOS detections (blue triangles). The dashed lines show $q = 30$ and 35 au for a reference. The vertical columns of model objects correspond to the mean motion resonances with Neptune (e.g., 7:3 at 52.9 au, 5:2 at 55.4 au, 8:3 at 57.9 au).

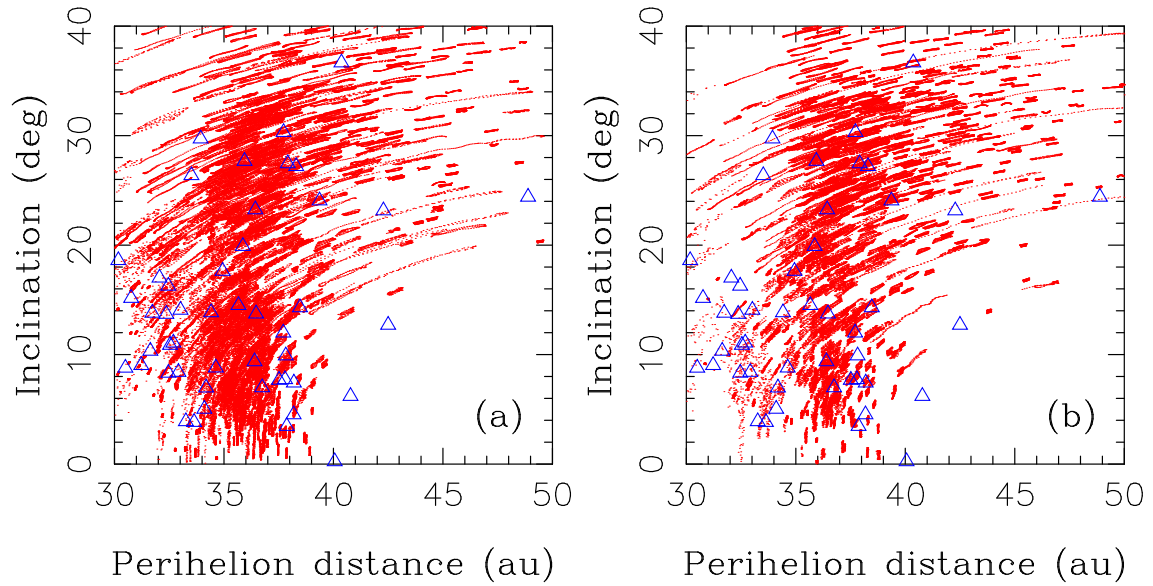


Fig. 2.— The orbital inclinations and perihelion distances of KBOs with $50 < a < 60$ au: dynamical models s10/30j in panel a and s30/100j in panel b (red dots; $e_N = 0.1$, Nesvorný et al. 2020). The model orbits are shown in the time interval of 10 Myr around the present epoch. The blue triangles are KBOs detected by OSSOS (Bannister et al. 2018).

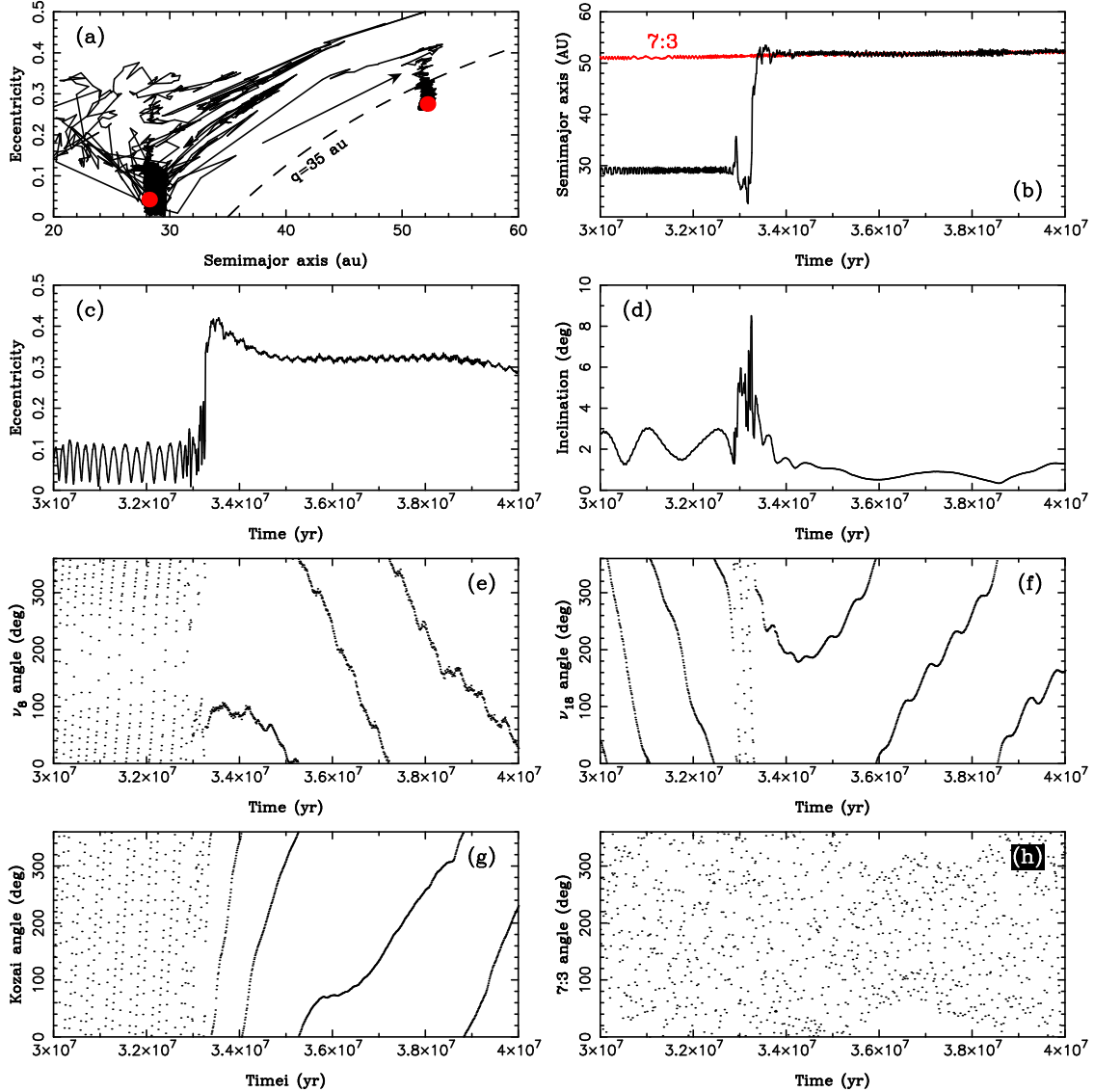


Fig. 3.— The orbital history of a test body that started below 30 au and ended on a detached, low-inclination orbit with $a \simeq 52$ au (model s10/30j with $e_N = 0.1$ from Nesvorný et al. 2020). The red dots in panel (a) show the initial and final orbits. The red line in panel (b) is the 7:3 resonance with Neptune. Various resonant angles are shown in panels (e)-(h): the ν_8 resonance angle $\varpi - \varpi_N$, where ϖ and ϖ_N are the perihelion longitudes (panel e), the ν_{18} resonance angle $\Omega - \Omega_N$, where Ω and Ω_N are the nodal longitudes (panel f), the Kozai resonance angle ω , where ω is the perihelion argument (panel g), and the 7:3 resonance angle $7\lambda - 3\lambda_N - 4\varpi$, where λ and λ_N are the mean longitudes (panel h).

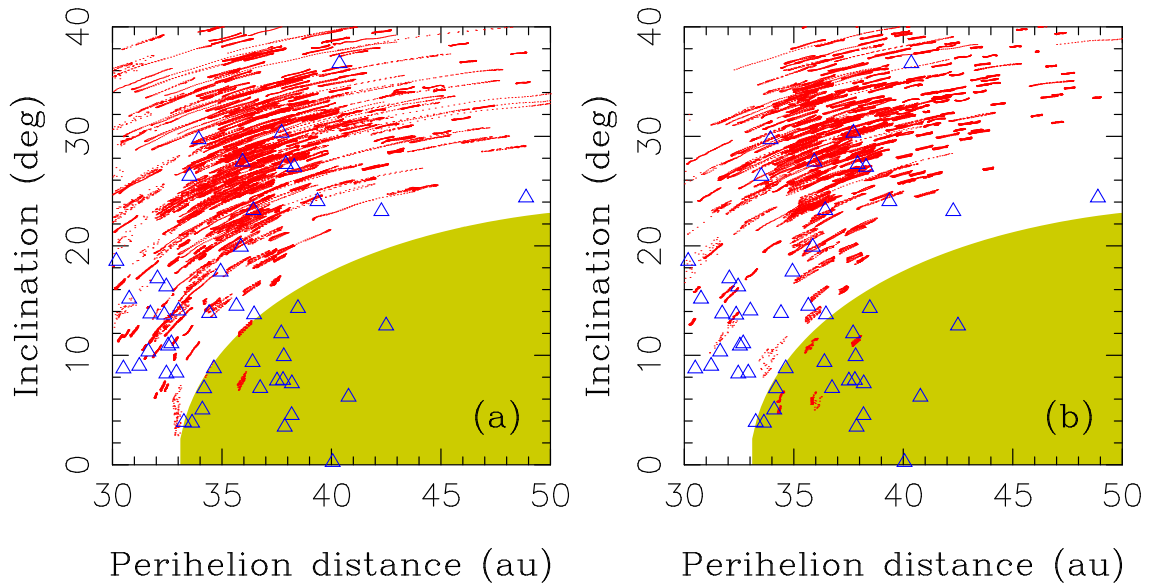


Fig. 4.— The orbital inclinations and perihelion distances of KBOs with $50 < a < 60$ au: dynamical models s10/30j in panel a and s30/100j in panel b (red dots; $e_N = 0-0.02$, Nesvorný et al. 2020). The model orbits are shown in the time interval of 10 Myr around the present epoch. The blue triangles are KBOs detected by OSSOS (Bannister et al. 2018). The shaded area (light green/dark yellow) is the excluded region that cannot be reached by orbits evolving from $q \sim 30$ au by the Kozai cycles.

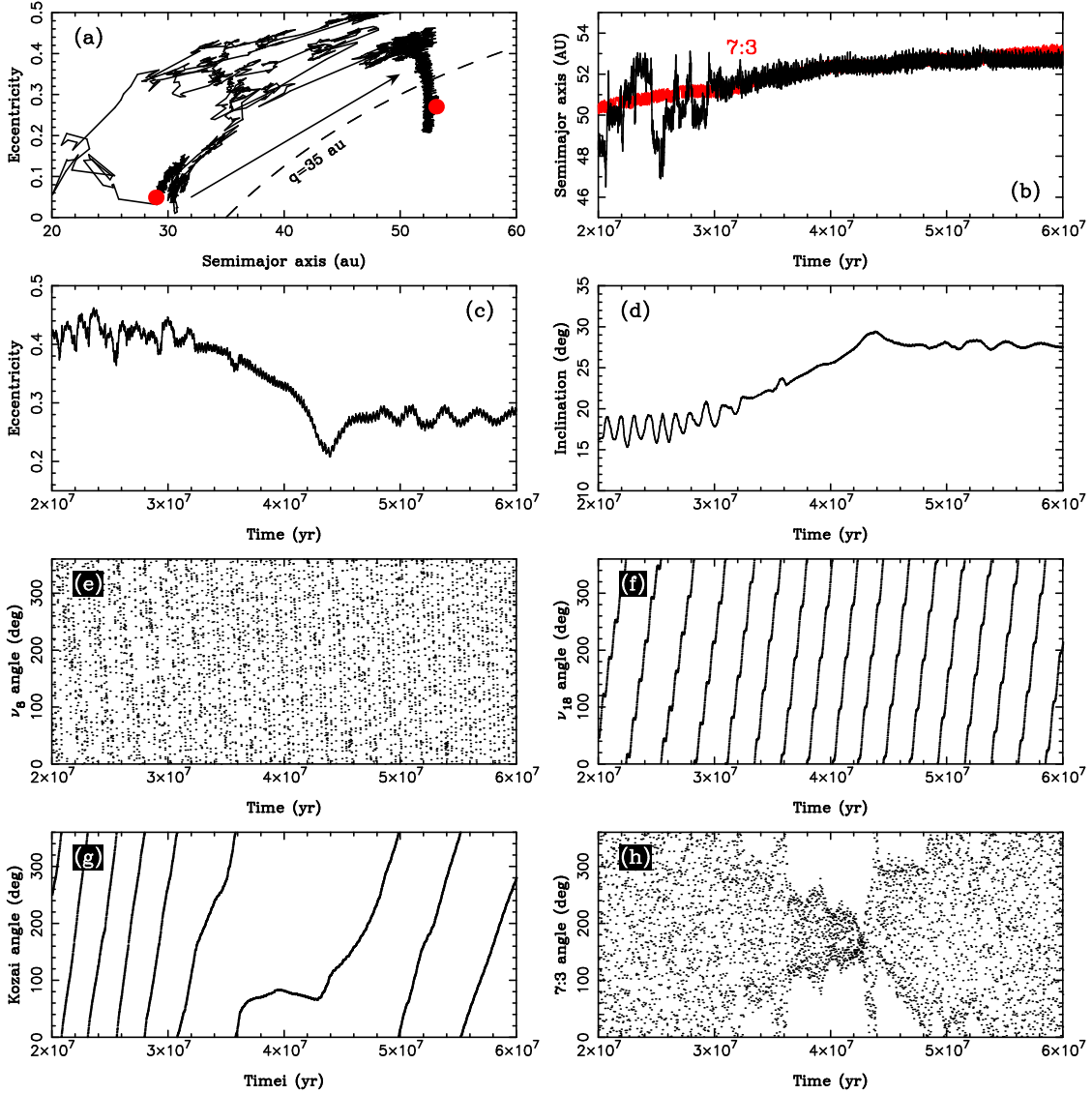


Fig. 5.— The orbital history of a test body that started below 30 au and ended on a detached, high-inclination orbit with $a \simeq 52.5$ au (model s10/30j with $e_N = 0.02$). See caption of Fig. 3 for a description of different panels. For the first ~ 30 Myr the body is kicked around by encounters with the outer planets (panel a). It then evolves, near $t = 36$ Myr, onto an orbit with a relatively small libration amplitude in the 7:3 resonance (panels b and h). This triggers an incomplete Kozai cycle with ω nearly reversing its rotation just after $t = 40$ Myr (panel g). As a result, the orbital eccentricity drops (panel c), the orbit becomes decoupled from Neptune, and the orbital inclination increases (panel d). The anti-correlated behavior of e and i is characteristic of the Kozai cycles (see main text). The orbit is eventually released from the migrating 7:3 resonance near $t = 55$ Myr (panel b).